Modelling excess properties of minerals and melts: implications for phase relations and seismic velocities in the Earth and other planetary bodies

R. Myhill

Bayerisches Geoinstitut, Universität Bayreuth, Universitätsstrasse 30, 95447 Bayreuth, Germany

Abstract

Thermodynamic models of solid and liquid solutions in the Earth Sciences are increasingly used to calculate phase relations and seismic properties over large pressure and temperature ranges. Research into mantle phase relations, subduction and differentiation of the early Earth frequently involves calculations spanning 1000s of K and 10s of GPa. Despite spanning such huge ranges, a common approximation is that excess thermodynamic derivatives within solid solutions (entropy and volume) are constant with respect to pressure and temperature. This is generally not true. In particular, absolute excess volumes tend to decrease with increasing pressure. As a result, the constant volume approximation may have a significant effect on both phase relations and seismic velocities calculated from solution models.

This paper describes an extension to the subregular Margules mixing model which employs intermediate compounds to define the excess thermodynamic properties of solid solutions. Mathematical derivations are provided for excess properties (H^{ex}, S^{ex}, V^{ex}) and their pressure and temperature derivatives (K_T^{ex}, α^{ex}, Cp^{ex} etc.). Heuristics are suggested for intermediate compounds where individual thermodynamic properties are poorly constrained.

Examples of pyroxene, garnet and melt solutions show that inclusion of a

*Corresponding author: R. Myhill
Email address: myhill.bob@gmail.com (R. Myhill)

variable excess volume is vital to simulate observed phase relations and seismic velocities. Large deviations from predictions made by classical solution models are observed for garnets under transition zone pressures and metallic melts with light elements. The new solution model scheme will allow for a huge wealth of experimental data to be incorporated into models of solid solutions, and is expected to be important for geochemical and geophysical models of the Earth, Mars and the Moon.
Keywords: high pressure, excess properties

1. Introduction

Solution models are a vital part of estimating phase relations at high pressure and temperatures. Typically, experimental estimates of excess enthalpy $\mathcal{H}$, entropy $\mathcal{S}$ and volume $\mathcal{V}$ across a binary solution are fit to some functional form (often quadratic, cubic). Extensions to ternary and larger systems are then built from these binaries. Typically, these models result in a series of interaction parameters of the form

$$W_{ij} = W_{ij}^{\mathcal{H}} + W_{ij}^{\mathcal{V}} P + W_{ij}^{\mathcal{S}} T \tag{1}$$

Models described in this way have been extremely successful in describing the thermodynamic properties of solid solutions at crustal pressures and temperatures. Under such conditions, the linear pressure and temperature approximation in Equation 1 is perfectly reasonable, as deviations from constant volume and entropy excesses are small. However, thermodynamic models are now being extended over much larger pressure and temperature ranges (Stixrude and Lithgow-Bertelloni, 2011; Holland and Powell, 2011; Holland et al., 2013; de Koker et al., 2013). It is unlikely that excess properties will remain constant over these ranges. For example, imagine two crystal lattices (A_xO_y and B_xO_y) comprising cations with different ionic radii and field strengths. The properties of the cations (and anion) result in different unit cell volumes and compressibilities; typically the lattice with the larger cationic radius will have a large

volume and smaller bulk modulus (Anderson and Anderson, 1970). Now imagine a third lattice with intermediate composition ($[A_{1-z}B_z]_xO_y$). This lattice will typically exhibit distortions which result in a positive or negative excess volume, as a direct result of changing the average cation-anion bond length relative to the sum of the endmembers (Vegard's Law). It is reasonable to suggest that longer bonds will be more compressible, and that therefore a positive excess volume will result in a negative excess bulk modulus. The reverse is also true; shorter bonds are likely to be less compressible. Of course, compression in complex minerals is unlikely to be well-described by a simple isotropic change in bond length. Nevertheless, other compression mechanisms such as polyhedral rotation are likely to be affected in a similar way; in general, a smaller volume will reduce the flexibility of the structure.

Thermoelastic models are also increasingly being used to interpret seismic data in terms of the temperature and composition of the deep Earth. Studies have focussed on Earth's mantle (e.g. Davies et al., 2012; Mosca et al., 2012; Deschamps et al., 2012) and core (e.g. Sanloup et al., 2000, 2004), and with the successful deployment of seismometers may soon extend to Mars (Gudkova et al., 2014). Again, the bulk modulus imposed by the constant excess volume approximation may be a significant and unnecessary contributor to error in these studies, especially for metallic liquids, where excess volumes at low pressures are often very large.

The current study addresses the problems outlined above by introducing a simple adaptation of the subregular Margules mixing model, using intermediate compounds to describe the excess properties of the solid solution as a function of pressure and temperature. The added flexibility comes with a large increase in the number of free parameters, so useful heuristics are also provided for the cases where individual parameters are unknown. This new formulation should enable a large number of studies on elastic properties of solid solutions to be incorporated into thermodynamic models. This study also highlights the need for high quality equation of state and seismic velocity data for intermediate compositions within solid solutions.

2. Theory

2.1. The Extended Subregular Margules (ESM) model

The subregular Margules mixing model within a binary system A-B approximates excess Gibbs free energies at any given pressure and temperature as a cubic function of composition (Helffrich and Wood, 1989):

$$\mathcal{G}^{xs} = X_B(1 - X_B)\left(W_{AB}X_B + W_{BA}(1 - X_B)\right) \tag{2}$$

In the special case that $W_{AB} = W_{BA}$, the function is a quadratic. I can define the Gibbs interaction parameter in terms of the Gibbs free energy of a 50:50 intermediate compound (AB) and the endmembers A and B:

$$W^{\mathcal{G}}_{AB} = 4(\mathcal{G}_{AB} + T\mathcal{S}^{\text{conf}}_{AB}) - 2(\mathcal{G}_A + \mathcal{G}_B) \tag{3}$$

where $\mathcal{S}^{\text{conf}}_{AB}$ is the configurational entropy of the intermediate compound. In the more general case that $W_{AB} \neq W_{BA}$, Equation 2 can be thought of as two symmetric interaction parameters with contributions that depend on the composition. Two intermediate compounds (AB and BA) are then required to describe the properties of the solution (Figure 1).

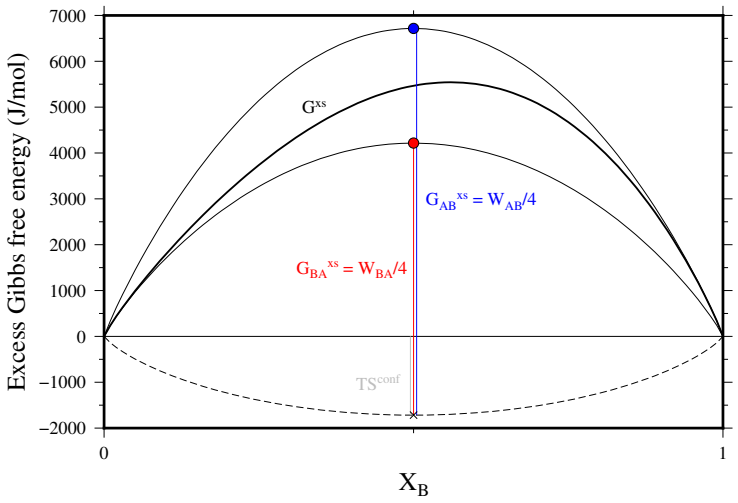

Figure 1: Schematic illustration of a binary subregular solution model.

Expanding the subregular solution model beyond a binary system, the excess nonconfigurational Gibbs free energy is (Helffrich and Wood, 1989)

$$\mathcal{G}^{xs} = \sum_{i=1}^{n}\sum_{j>1}^{n} X_i X_j \left(W_{ij}X_j + W_{ji}X_i + 0.5(W_{ij}+W_{ji}) \sum_{k}^{n} (1-\delta_{ik})(1-\delta_{jk})X_k \right) \tag{4}$$

Each of the individual W_{ij} terms in Equation 4 can be determined via the properties of an intermediate compound, just as described in the binary *A*-*B* system (Equation 2). The properties of the solid solution with composition X_i are then defined as follows:

$$\mathcal{G} = \sum_i X_i \mathcal{G}_i + \mathcal{G}^{xs} \tag{5}$$

$$\mathcal{H} = \sum_i X_i \mathcal{H}_i + \mathcal{H}^{xs} \tag{6}$$

$$\mathcal{S} = \sum_i X_i \mathcal{S}_i + \mathcal{S}^{xs} \tag{7}$$

$$\mathcal{V} = \sum_i X_i \mathcal{V}_i + \mathcal{V}^{xs} \tag{8}$$

$$C_P = \sum_i X_i C_P + T\left(\frac{\partial \mathcal{S}}{\partial T}\right)_P^{xs} \tag{9}$$

$$\alpha = \frac{1}{\mathcal{V}}\left(\sum_i X_i \alpha_i \mathcal{V}_i + \left(\frac{\partial \mathcal{V}}{\partial T}\right)_P^{xs}\right) \tag{10}$$

$$K_T = \frac{\mathcal{V}}{\sum_i \frac{X_i \mathcal{V}_i}{K_{Ti}} - \left(\frac{\partial \mathcal{V}}{\partial P}\right)_T^{xs}} \tag{11}$$

$$C_V = C_P - \mathcal{V} T \alpha^2 K_T \tag{12}$$

$$K_S = K_T \frac{C_P}{C_V} \tag{13}$$

$$\gamma = \frac{\alpha K_T \mathcal{V}}{C_V} \tag{14}$$

With the exception of the enthalpy excess, excess terms ($\mathcal{S}^{xs}$, $\mathcal{V}^{xs}$ etc) are derived in the same way as the excess Gibbs free energy (Equation 4), with interaction terms defined as follows:

$$W_{ij}^{\mathcal{S}} = 4(\mathcal{S}_{ij} - \mathcal{S}_{ij}^{\text{conf}}) - 2(\mathcal{S}_i + \mathcal{S}_j) \tag{15}$$

$$W_{ij}^{\mathcal{V}} = 4\mathcal{V}_{ij} - 2(\mathcal{V}_i + \mathcal{V}_j) \tag{16}$$

$$W_{ij}^{\partial\mathcal{V}/\partial P} = -4\mathcal{V}_{ij}/K_{Tij} + 2(\mathcal{V}_i/K_{Ti} + \mathcal{V}_j/K_{Tj}) \tag{17}$$

$$W_{ij}^{\partial\mathcal{V}/\partial T} = 4\alpha_{ij}\mathcal{V}_{ij} - 2(\alpha_i\mathcal{V}_i + \alpha_j\mathcal{V}_j) \tag{18}$$

$$W_{ij}^{\partial\mathcal{S}/\partial T} = \frac{4C_{Pij} - 2(C_{Pi} + C_{Pj})}{T} \tag{19}$$

Finally, excess enthalpy is defined as

$$\mathcal{H}^{xs} = \mathcal{G}^{xs} + T\mathcal{S}^{xs} \tag{20}$$

2.2. Heuristics

It is often the case that endmembers are particularly well studied, while the properties of the solid solution are constrained only by enthalpies of solution and volumes at room temperature and pressure. The remaining properties of the intermediate compounds must be estimated by the user. In this study, we suggest that the following heuristics be used:

$$\mathcal{S}_{ij} = 0.5(\mathcal{S}_i + \mathcal{S}_j) + \mathcal{S}_{ij}^{\text{conf}} \tag{21}$$

$$C_{Pij} = 0.5(C_{Pi} + C_{Pj}) \tag{22}$$

$$\alpha_{ij} = 0.5\mathcal{V}\left(\frac{\alpha_i}{\mathcal{V}_i} + \frac{\alpha_j}{\mathcal{V}_j}\right) \tag{23}$$

$$K'_T = -\frac{\partial}{\partial P}\left(\mathcal{V}\left(\frac{\partial P}{\partial \mathcal{V}}\right)_T\right) \sim \mathcal{V}\left(\sum_i \frac{X_i\mathcal{V}_i}{K'_{Ti}+1}\right)^{-1} - 1 \tag{24}$$

If excess volumes are zero, it is likely that they will remain zero as temperatures and pressures increase. In this case, the bulk modulus is given by Equation 11, with the differential term equal to zero. In contrast, non-zero excess volumes are unlikely to remain constant with pressure and temperature. I suggest that, in the absence of other data a useful heuristic is $\left(\frac{\partial\mathcal{V}}{\partial P}\right)_T^{xs} \to 0$ as $P \to \infty$.

A useful way to view the change in bulk modulus across a solid solution is to compare the excess bulk modulus to that implied by the $K_TV = constant$ rule of thumb proposed by Anderson and Anderson (1970) to estimate the compressibility of endmembers based on their molar volumes. The heuristic we propose in this study predicts a larger excess term than that suggested by the rule of thumb, which we describe using a factor ξ:

$$K_T \sim 0.5(K_{Ti} + K_{Tj}) + \xi \left(\frac{K_{Ti}\mathcal{V}_j + K_{Tj}\mathcal{V}_j}{2\mathcal{V}} - 0.5(K_{Ti} + K_{Tj}) \right) \qquad (25)$$

Typically, a value of ∼6 provides a useful estimate of ξ.

Now that we have described the new model and heuristics related to the construction of intermediate compounds, we turn to a few geologically relevant examples. The models in this study are all implemented in the open software *burnman*, a mineral physics toolkit written in python. The software, first described in Cottaar et al. (2014), was originally designed for seismic velocity calculations. It has since been augmented with thermodynamics functionality, including a range of different models for solid solutions.

3. Examples

3.1. Pyroxene

Our first example is that of jadeite-aegirine pyroxene, an almost ideal solid solution (from a volumetric perspective). I use this model to illustrate that even when excess volumes are extremely small, excess bulk moduli are resolvable. The experimental data is that of Nestola et al. (2006), and the equation of state used is the Modified Tait (Holland and Powell, 2011). The fit to the volume data is shown in Figure 2.

Table 1: Jadeite-Aegirine mixing parameters to fit the room temperature data of Nestola et al. (2006). The K_0' for the intermediate compound is fixed to the value given by the heuristic proposed in the text. $K_0'' = -K_0'/K_0$.

	jadeite	aegirine	$jd_{50}ae_{50}$	$ae_{50}jd_{50}$
V_0 (cm^3/mol)	60.5640 ± 0.0001	64.6261 ± 0.0004	62.3641 ± 0.0005	62.4522 ± 0.0005
K_0 (GPa)	133.5 ± 0.2	116.0 ± 0.2	124.8 ± 0.5	126.7 ± 0.4
K_0'	4.6 [fixed]	4.4 [fixed]	4.4785 [heuristic]	4.4785 [fixed]

Using the derived properties of the solid solution, we can fit the excess volume as a function of pressure (Figure 3). The decay of excess volume as a function

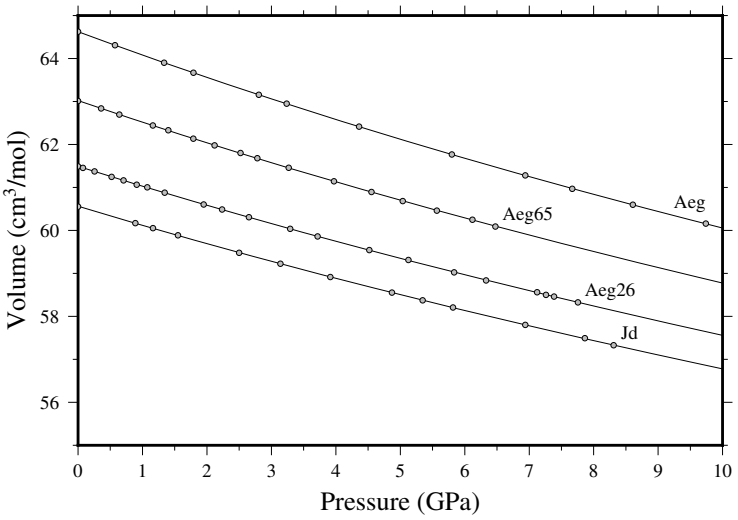

Figure 2: Pressure-volume data in the binary system Jadeite-Aegirine (Nestola et al., 2006), with the model proposed in this study.

of pressure is in excellent agreement with the prediction that excess volumes decay to zero at extreme pressures. For the 50:50 intermediate, our excess bulk moduli and volumes indicate that $\xi \sim 11$ (Equation 25).

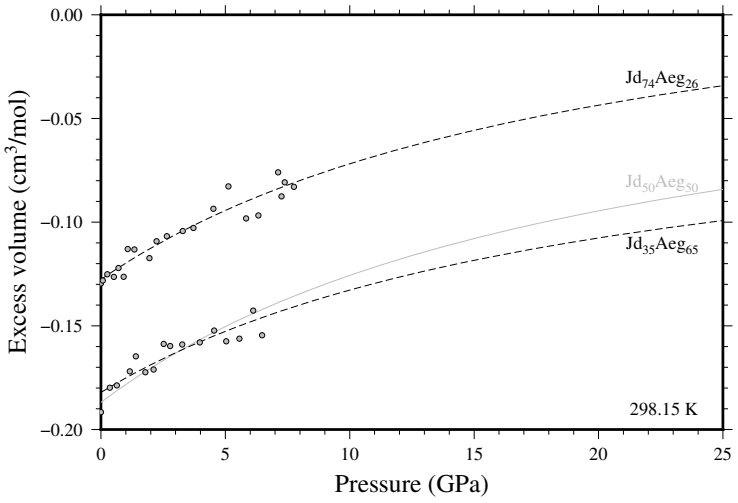

Figure 3: Excess volume for Jd-Aeg pyroxenes calculated from our model.

3.2. Garnet

Our second example is the pyrope-grossular join, which is well-known to have significant non-ideality and volumes of mixing (Newton et al., 1977; Bosenick and Geiger, 1997; Ganguly et al., 1996). Recently, it has been suggested that the excess volumes of mixing are $\sim$1 cm^3/mol, 2–3 times larger than previously suggested, and associated with very large negative excess bulk moduli (Du et al., 2015). It is proposed that the differences are due to a hydrogrossular component in the crystals synthesised in piston cylinder apparatus in earlier studies, which becomes unstable at high pressures.

Here, we create four models to describe the room temperature equations of state for the pyrope-grossular system using the pyrope and grossular endmembers from Holland and Powell (2011). Two models are presented for the data of (Du et al., 2015), to describe the reported behaviour close to the center and at the edges of the solid solution. The third model is the constant volume subregular Margules model of Ganguly et al. (1996). A fourth model has the same excess volume as Ganguly et al. (1996), but a negative excess bulk modulus which allows the excess volume to decay to zero at high pressures ($\xi = 6$). The standard state bulk moduli are shown in Figure 4.

It is immediately obvious that the bulk moduli calculated from the Du et al. (2015) study exhibit very large deviations from a linear trend. The symmetric curve derived from the two compounds in the middle of the binary yields $\xi = 10$, a value which is not unreasonable, and results in a change in sign of the volume excess at 20–25 GPa. In contrast, the trend derived from the compounds with 20% and 80% pyrope content yields $\xi = 52$. This extreme value leads to negative excess volumes at 5–6 GPa, which does not seem to be very likely. To avoid this, K'_T must be increased to >20, which is also extremely unlikely.

The trend calculated from the terms in Ganguly et al. (1996) has a small positive excess bulk modulus, which is always the case where $\mathcal{V}^{xs}$ is held fixed. For the reasons outlined in the introduction, this is probably unlikely. The final model, constructed using the heuristics described in the previous section yields an excess bulk modulus on the order of 2–3 GPa.

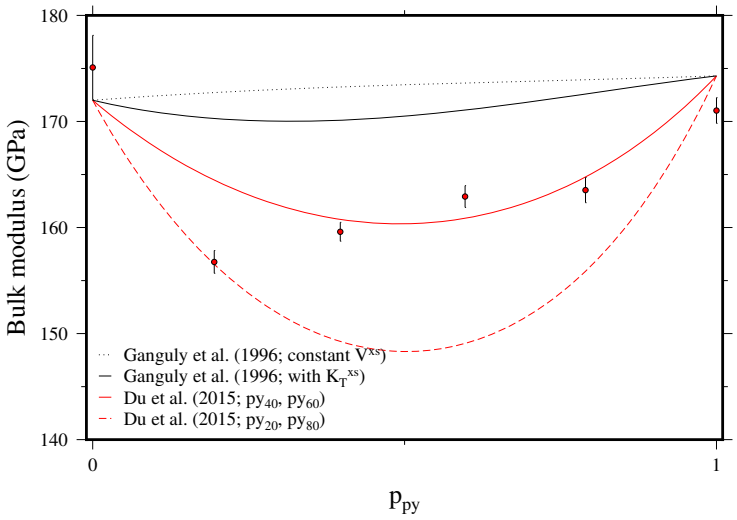

Figure 4: Bulk moduli in the binary system Pyrope-Grossular (Du et al., 2015), with the models proposed in this study.

These models are now used to illustrate the effect of decaying excess volumes on seismic wave velocities. P-wave, S-wave and bulk sound velocities are functions of isentropic bulk and shear moduli and density:

$$V_P = \sqrt{\frac{K_S + \frac{4}{3}G}{\rho}} \tag{26}$$

$$V_S = \sqrt{\frac{G}{\rho}} \tag{27}$$

$$V_\Phi = \sqrt{\frac{K_S}{\rho}} \tag{28}$$

Thermodynamic solution models say nothing about shear moduli, so we restrict our discussion to the bulk sound velocity. Figure 5 shows the bulk sound velocity at ambient temperature for the four solid solution models in the text. The models of Du et al. (2015) result in large depressions of bulk sound velocity. The model constructed from the py_{40} and py_{60} samples results in a 4% depression relative to the constant $\mathcal{V}^{xs}$ case throughout the upper mantle pressure range. In contrast, the model based on the excess volume model proposed in Ganguly et al. (1996) predicts a 1% decrease in bulk sound speed.

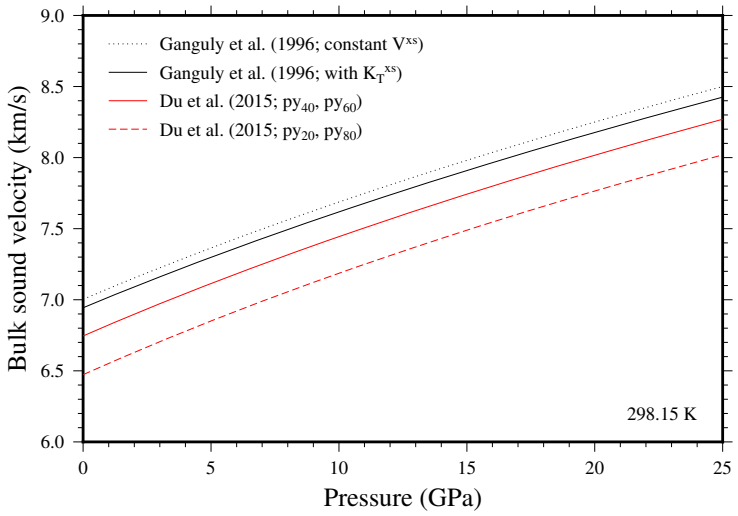

Figure 5: Bulk sound velocities of $Py_{50}Gr_{50}$ at room temperature according to the fixed excess volume model of (Ganguly et al., 1996), a modified model incorporating an excess bulk modulus, and the two models derived from Du et al. (2015).

At present, it is not easy to state with certainty whether natural garnets have P-V-T equations of state similar to those suggested by Du et al. (2015), or similar to those in previous studies (Newton et al., 1977; Bosenick and Geiger, 1997; Ganguly et al., 1996). If a hydrogrossular component is indeed the cause for low excess volumes in piston cylinder-synthesised garnets, then garnets in the mantle are likely to have relatively high volume excesses and low bulk moduli. In this case, constant V^{xs} models are clearly inappropriate both for calculations of mantle phase relations and seismic velocities. Nevertheless, even in the case of the model derived from Ganguly et al. (1996), phase relations are still likely to be affected noticably by the change in excess volume with pressure. At the conditions where garnet finally breaks down, the differences in free energy between models are on the order of kilojoules. Accurately constraining the elastic properties of solid solutions should be a key goal both for seismic velocity calculations and for thermodynamics.

3.3. Fe-FeO melt

Our final example is that of Fe-FeO melt. As oxygen may be one of the more abundant light elements in the core, understanding the thermodynamics of this liquid solution is an important part of understanding mantle-core differentiation and interaction over billions of years. At pressures <25 GPa, the Fe-FeO solution exhibits signficant non-ideality, with a large miscibility gap between ionic and metallic Fe-O liquids (Kowalski and Spencer, 1995; Tsuno et al., 2007; Frost et al., 2010). As pressure increases, this miscibility gap disappears, indicating a negative excess volume of mixing (Figure 6). To explain the increase in eutectic temperature with pressure, Komabayashi (2014) suggest that mixing becomes essentially ideal at >100 GPa.

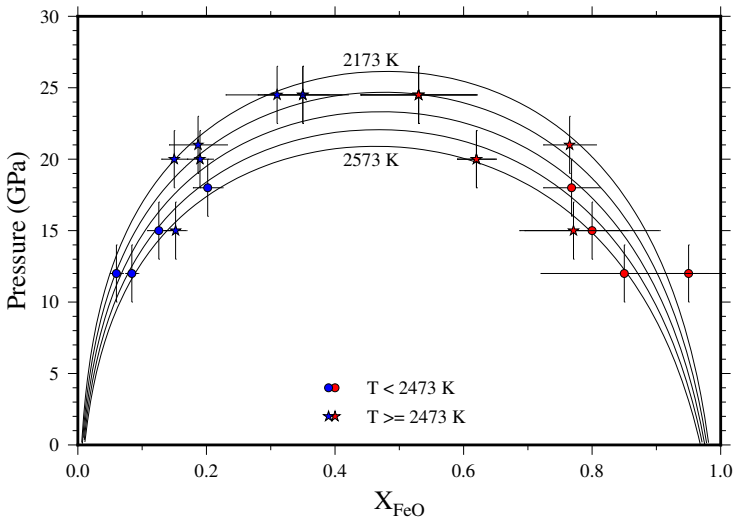

Figure 6: Fe-O solvus

To model processes of mantle differentiation and core formation, it would be extremely useful to have a single model describing the properties of melts over relevant pressure and temperature ranges. Clearly a high pressure ideal model cannot be reconciled with a low pressure model with large excess volumes of mixing without incorporating excess bulk moduli and thermal expansivities. Below ∼25 GPa, the properties of the liquid can be estimated using the compositions

of coexisting metallic and ionic liquid (Tsuno et al., 2007; Frost et al., 2010). The chemical potentials of Fe and FeO are equal in the ionic and metallic liquids, providing the two constraints necessary to estimate Margules parameters at each pressure and temperature (Figure 7).

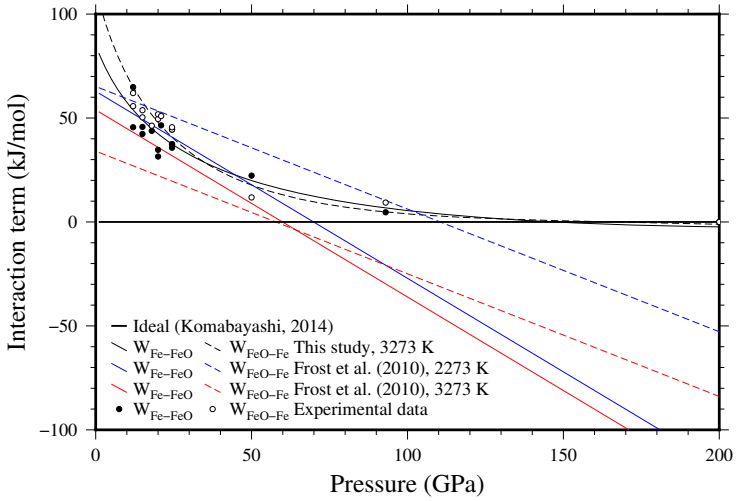

Figure 7: Interaction terms in Fe-FeO melt as a function of pressure.

At >25 GPa, the pressure, temperature and compositions of eutectic liquid at high pressure (Seagle et al., 2008) provide further constraints, providing we know the relative Gibbs free energies of liquid and solid Fe and FeO. Here, we fit the thermodynamic properties of the FCC and HCP iron endmembers and of B1 FeO to published P-V-T data and phase boundaries. The liquid endmembers are fit with available room pressure data, and the effect of pressure is estimated using constraints on the melting curves from Anzellini et al. (2013), Seagle et al. (2008) and Ozawa et al. (2011). The uncertainties on composition and temperature of the eutectic are rather large, so these data are supplemented by the requirement that excess volumes become zero at very high pressure. The parameters used to create the fits in Figures 7 and 8 are given in Table 2. In this work, we fix excess entropy and thermal expansion to zero. The majority of the <25 GPa data was collected within a ∼200 K temperature range, and is associated with similar temperature uncertainties, which introduces very large uncertainties in

excess entropies. Add to that the possibility of phase separation during quench and the large uncertainty in coexisting ionic/metallic melt compositions, there is no clear evidence for the large temperature dependence proposed by Frost et al. (2010), although they do slightly improve the fit to the data (mostly by increasing the pressure at which the solvus closes at high temperature).

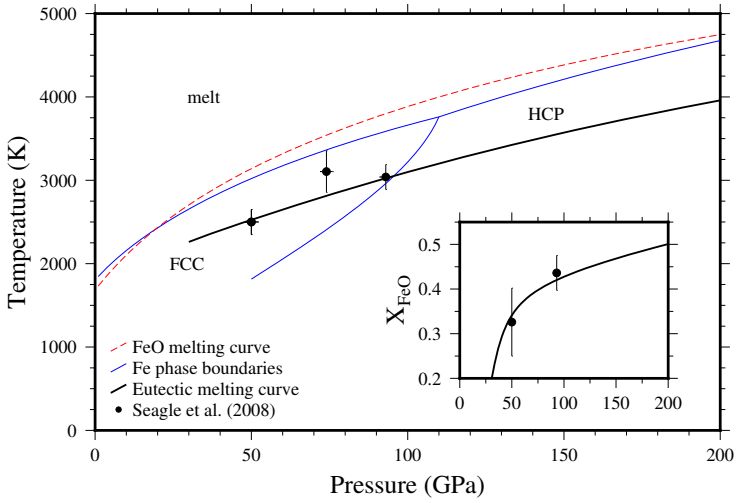

Figure 8: Melting temperature in the Fe-O system as a function of pressure. Inset: eutectic composition in the Fe-O system.

Table 2: Excess Fe-FeO mixing parameters to fit the data in Figures 7 and 8 at a reference temperature of 1809 K and pressure of 50 GPa.

Property	$Fe_{50}FeO_{50}$	$FeO_{50}Fe_{50}$
H^{xs} (J/mol)	5000 ± 400	4400 ± 400
S^{xs} (J/K/mol)	0 [fixed]	0 [fixed]
V^{xs} (cm^3/mol)	-0.117 ± 0.009	-0.136 ± 0.009
K^{xs} (GPa)	28 ± 5	45 ± 5
K'^{xs}	-0.07 ± 0.12	-0.37 ± 0.12
a^{xs}	0 [fixed]	0 [fixed]

4. Conclusions

The use of intermediate compounds to describe excess properties is an extremely simple but powerful concept that lends a great deal of flexibility to models without necessarily increasing the number of parameters which need to be fit to the available experimental data. I note that the equations derived here are all quite general, and therefore easily applicable to a wide range of different equations of state.

The heuristics suggested here place constraints on seismic properties which are significantly more strict than typical uncertainties on bulk moduli derived from ultrasonic interferometry, Brillouin scattering or static compression. For example, along the pyrope-majorite join, excess volumes are small (0.1 cm^3/mol) (Heinemann et al., 1997). With the assumption that excess volumes decrease to zero with increasing pressure, the excess bulk modulus is constrained to be $\sim$-0.6 GPa. In comparison, the range in bulk modulus estimates anywhere along the pyrope-majorite join is about 10 GPa (see, for example Hunt et al., 2010). So far, high pressure elasticity studies have mostly been focussed on binary joins with small excess volumes at ambient pressure (Fan et al., 2015; Huang and Chen, 2014). That they should exhibit small excess bulk moduli is in excellent agreement with the heuristics proposed here, but a far more rigorous test would be to investigate systems with large volume excesses.

It is envisaged that the model formulation proposed in this study will be very useful in modelling silicate and metallic melts, where excess volumes are large at low pressure. Even in the MgO-SiO_2 system, excess entropies and volumes are strongly dependent on temperature and pressure (de Koker et al., 2013). Finally, this model allows for much greater freedom in adjusting the shapes of free energy curves as a function of pressure and temperature, which should be extremely useful for phase equilibria studies, especially those investigating chemical potentials and fugacities which depend greatly on the compositional gradient of the free energy curve.

5. Acknowledgments

RM is funded by the Advanced ERC Grant awarded to the "ACCRETE" project (Contract number 290568). He would like to thank Dave Rubie, Dan Frost and Christopher Beyer for useful discussions.

References

Anderson, D.L., Anderson, O.L., 1970. Brief report: The bulk modulus-volume relationship for oxides. Journal of Geophysical Research 75, 3494–3500.

Anzellini, S., Dewaele, A., Mezouar, M., Loubeyre, P., Morard, G., 2013. Melting of Iron at Earth's Inner Core Boundary Based on Fast X-ray Diffraction. Science 340, 464–466.

Bosenick, A., Geiger, C.A., 1997. Powder x ray diffraction study of synthetic pyrope-grossular garnets between 20 and 295 k. Journal of Geophysical Research: Solid Earth 102, 22649–22657.

Cottaar, S., Heister, T., Rose, I., Unterborn, C., 2014. BurnMan: A lower mantle mineral physics toolkit. Geochemistry, Geophysics, Geosystems 15, 1164–1179.

Davies, D.R., Goes, S., Davies, J., Schuberth, B., Bunge, H.P., Ritsema, J., 2012. Reconciling dynamic and seismic models of earth's lower mantle: The dominant role of thermal heterogeneity. Earth and Planetary Science Letters 353-354, 253 – 269.

de Koker, N., Karki, B.B., Stixrude, L., 2013. Thermodynamics of the MgO-SiO_2 liquid system in Earth's lowermost mantle from first principles. Earth and Planetary Science Letters 361, 58–63.

Deschamps, F., Cobden, L., Tackley, P.J., 2012. The primitive nature of large low shear-wave velocity provinces. Earth and Planetary Science Letters 349350, 198 – 208.

Du, W., Clark, S.M., Walker, D., 2015. Thermo-compression of pyrope-grossular garnet solid solutions: Non-linear compositional dependence. American Mineralogist 100, 215–222.

Fan, D., Xu, J., Ma, M., Liu, J., Xie, H., 2015. Pvt equation of state of spessartinealmandine solid solution measured using a diamond anvil cell and

in situ synchrotron x-ray diffraction. Physics and Chemistry of Minerals 42, 63–72.

Frost, D.J., Asahara, Y., Rubie, D.C., Miyajima, N., Dubrovinsky, L.S., Holzapfel, C., Ohtani, E., Miyahara, M., Sakai, T., 2010. Partitioning of oxygen between the Earth's mantle and core. Journal of Geophysical Research (Solid Earth) 115, 2202.

Ganguly, J., Cheng, W., Tirone, M., 1996. Thermodynamics of aluminosilicate garnet solid solution: new experimental data, an optimized model, and thermometric applications. Contributions to Mineralogy and Petrology 126, 137–151.

Gudkova, T., Lognonné, P., Zharkov, V., Raevsky, S., 2014. On the scientific aims of the miss seismic experiment. Solar System Research 48, 11–21.

Heinemann, S., Sharp, T.G., Seifert, F., Rubie, D.C., 1997. The cubic-tetragonal phase transition in the system majorite ($Mg_4Si_4O_{12}$) - pyrope ($Mg_3Al_2Si_3O_{12}$), and garnet symmetry in the Earth's transition zone. Physics and Chemistry of Minerals 24, 206–221.

Helffrich, G., Wood, B.J., 1989. Subregular model for multicomponent solutions. American Mineralogist 74, 1016–1022.

Holland, T.J., Hudson, N.F., Powell, R., Harte, B., 2013. New thermodynamic models and calculated phase equilibria in ncfmas for basic and ultrabasic compositions through the transition zone into the uppermost lower mantle. Journal of Petrology 54, 1901–1920.

Holland, T.J.B., Powell, R., 2011. An improved and extended internally consistent thermodynamic dataset for phases of petrological interest, involving a new equation of state for solids. Journal of Metamorphic Geology 29, 333–383.

Huang, S., Chen, J., 2014. Equation of state of pyrope-almandine solid solution measured using a diamond anvil cell and in situ synchrotron X-ray diffraction. Physics of the Earth and Planetary Interiors 228, 88–91.

Hunt, S.A., Dobson, D.P., Li, L., Weidner, D.J., Brodholt, J.P., 2010. Relative strength of the pyropemajorite solid solution and the flow-law of majorite containing garnets. Physics of the Earth and Planetary Interiors 179, 87 – 95.

Komabayashi, T., 2014. Thermodynamics of melting relations in the system Fe-FeO at high pressure: Implications for oxygen in the Earth's core. Journal of Geophysical Research (Solid Earth) 119, 4164–4177.

Kowalski, M., Spencer, P., 1995. Thermodynamic reevaluation of the C-O, Fe-O and Ni-O systems: Remodelling of the liquid, BCC and FCC phases. Calphad 19, 229 – 243.

Mosca, I., Cobden, L., Deuss, A., Ritsema, J., Trampert, J., 2012. Seismic and mineralogical structures of the lower mantle from probabilistic tomography. Journal of Geophysical Research: Solid Earth 117, n/a–n/a. B06304.

Nestola, F., Boffa Ballaran, T., Liebske, C., Bruno, M., Tribaudino, M., 2006. High-pressure behaviour along the jadeite $NaAlSi_2O_6$-aegirine $NaFeSi_2O_6$ solid solution up to 10 GPa. Physics and Chemistry of Minerals 33, 417–425.

Newton, R.C., Charlu, T.V., Kleppa, O.J., 1977. Thermochemistry of high pressure garnets and clinopyroxenes in the system CaO-MgO-Al_2O_3-SiO_2. Geochimica et Cosmochimica Acta 41, 369–377.

Ozawa, H., Takahashi, F., Hirose, K., Ohishi, Y., Hirao, N., 2011. Phase Transition of FeO and Stratification in Earth's Outer Core. Science 334, 792–.

Sanloup, C., Fiquet, G., Gregoryanz, E., Morard, G., Mezouar, M., 2004. Effect of Si on liquid Fe compressibility: Implications for sound velocity in core materials. Geophysical Research Letters 31, 7604.

Sanloup, C., Guyot, F., Gillet, P., Fiquet, G., Mezouar, M., Martinez, I., 2000. Density measurements of liquid Fe-S alloys at high-pressure. Geophysical Research Letters 27, 811–814.

Seagle, C.T., Heinz, D.L., Campbell, A.J., Prakapenka, V.B., Wanless, S.T., 2008. Melting and thermal expansion in the Fe-FeO system at high pressure. Earth and Planetary Science Letters 265, 655–665.

Stixrude, L., Lithgow-Bertelloni, C., 2011. Thermodynamics of mantle minerals - II. Phase equilibria. Geophysical Journal International 184, 1180–1213.

Tsuno, K., Ohtani, E., Terasaki, H., 2007. Immiscible two-liquid regions in the Fe O S system at high pressure: Implications for planetary cores. Physics of the Earth and Planetary Interiors 160, 75–85.